

Received August 23, 2019, accepted September 8, 2019, date of publication October 8, 2019, date of current version October 23, 2019.

Digital Object Identifier 10.1109/ACCESS.2019.2946265

Power Quality Improvement in Microgrids Under Critical Disturbances Using an Intelligent Decoupled Control Strategy Based on Battery Energy Storage System

JABER ALSHEHRI¹, (Student Member, IEEE), AND MUHAMMAD KHALID^{1,2}, (Member, IEEE)

¹Electrical Engineering Department, King Fahd University of Petroleum and Minerals, Dhahran 31261, Saudi Arabia

²K.A.CARE Energy Research and Innovation Center, Dhahran 31261, Saudi Arabia

Corresponding author: Jaber Alshehri (jaber.a.shehri@gmail.com)

This work was supported by the Deanship of Research (DSR) at the King Fahd University of Petroleum and Minerals (KFUPM) under Project RG171009. The work of M. Khalid was supported by the King Abdullah City for Atomic and Renewable Energy (K.A. CARE).

ABSTRACT The concept of microgrids (MGs) provides the flexibility to integrate renewables into the power network. Nevertheless, the transience of most renewable energy sources (RESs) exacerbates the power quality of the grid network. Furthermore, the unpredictability of RESs additionally becomes challenging in case of high magnitude disturbances. The deployment and optimal utilization of energy storage systems, to act as an energy buffer are hence pertinent. In this paper, a control strategy for a battery energy storage system (BESS) is formulated based on two intelligent decoupled controllers. The objective is the restoration of system voltage and frequency considering a wide range of disturbances and hence circumvent the power quality degradation. The proposed controller is based on hybrid differential evolution optimization and artificial neural network (DEO-ANN). The controller parameters are tuned online by training the ANN with the sets of input and output data obtained during the process of optimizing the two controllers under low and high disturbances using DEO. Finally, the effectiveness of the proposed controller is validated on a power network consisting of a synchronous generator, photovoltaic power system, and BESS. The simulation results prove the robustness of the proposed control approach as compared with a benchmark controller.

INDEX TERMS Artificial neural networks, battery energy storage systems, differential evolution optimization, intelligent decoupled controllers, microgrids, photovoltaic system, power quality improvement, proportional-integral controller, synchronous generator.

NOMENCLATURE

A. ABBREVIATIONS

ANNs	Artificial neural networks
BESS	Battery energy storage system
DEO	Differential evolution optimization
DERs	Distributed energy resources
DG	Distributed generation
EAs	Evolutionary algorithms
EP	Evolutionary programming
ES	Evolution strategy
ESDs	Energy storage devices
ESS	Energy storage system

FCs	Fuel cells
FESS	Flywheel energy storage system
FL	Fuzzy logic
FR	Frequency restoration
GA	Genetic algorithm
GP	Genetic programming
GTs	Gas turbines
HIL	Hardware-in-loop
HTs	Hydropower turbines
ICE	Internal combustion engine
IGBT	Insulated-gate bipolar transistor
ISE	Integral squared error
LP	Low pass
MG	Microgrid

The associate editor coordinating the review of this manuscript and approving it for publication was Amedeo Andreotti¹.

PCC	Point of common coupling
PI	Proportional-integral
PID	Proportional-integral-derivative
PSO	Particle swarm optimization
PV	Photovoltaic system
PWM	Pulse-width modulation
RESs	Renewable energy sources
RPS	Reactive power sharing
SCCESS	Super-capacitor energy storage system
SG	Synchronous generator
SLD	Single line diagram
SMES	Superconducting magnetic energy storage
VSC	Voltage source converter
VSI	Voltage source inverter
WT	Wind turbine

V_{cpq}	LP filter capacitor voltage in q-axis
i_{pd}	LP filter output current in d-axis
i_{pq}	LP filter output current in q-axis
V_{dcs}	Battery DC linking capacitor voltage
i_{std}	BESS output current in d-axis
i_{stq}	BESS output current in q-axis
m_B	Battery-VSC modulation index
ψ_B	Battery-VSC phase angle

B. PARAMETERS

ω_0	Reference angular frequency
H	Inertia constant
T'_{d0}	Open circuit field constant
x_d	D-axis synchronous reactance
x'_d	D-axis transient reactance
τ_E	Exciter time constant
α_E	Exciter gain
V_{g0}	SG reference terminal voltage
E_{fd0}	Reference field voltage in d-axis
L_b	Boost converter inductor
d_{pv}	Boost converter duty ratio
C_{dcpv}	DC linking capacitor
R_{pf}	LP Filter resistance
L_{pf}	LP Filter inductance
R_{pdr}	Damping resistor
R_p	Transmission line coupling resistance
L_p	Transmission line coupling inductance
C_{pf}	LP Filter capacitor
R_B	Battery storage resistance
C_{dcs}	DC linking capacitance
R_{st}	Resistance of VSC
L_{st}	Inductance of VSC
V_0	Reference PCC bus voltage

C. VARIABLES

δ	Angular displacement
ω	Angular frequency
E_{fd}	Field voltage in d-axis
e'_q	Internal voltage in q-axis
P_e	Output electrical power
P_m	Input mechanical power
i_{PV}	PV cell output current
V_{dcpv}	PV DC linking capacitor voltage
i_{pfd}	VSI output current in d-axis
i_{pfq}	VSI output current in q-axis
m_{PV}	PV-VSI modulation index
ψ_{PV}	PV-VSI phase angle
V_{cpd}	LP filter capacitor voltage in d-axis

I. INTRODUCTION

The limited resources for conventional power generation in combination with environmental concern has brought about the need for integrating renewable energy resources (RESs) into the existing power grid, such as photovoltaics (PVs), wind turbines (WTs) and hydropower turbines (HTs) [1]. The consolidation of RESs has significantly changed the structural topology of conventional power networks from centralized power generation to distributed generation (DG); typically, small-scale power generations that lie in the close proximity to the load centers [2]. The power quality and reliability of conventional radial distribution networks in several countries have degraded. In accordance, the concept of micro-grid (MG) is adopted to obviate and circumvent these network deficiencies [3], [4]. Small-scale power generation systems (PV, WT, etc.), loads and energy storage devices (ESDs) are typically the general attributes of MG [5]–[7]. MGs can be operated on either grid-connected mode or islanded mode [8]. The control requirements vary, based on the operating mode and the controlled components such as DGs, ESDs and loads [9]. The small-scale DGs can be categorized on the basis of their grid interface as, inertial type or inverter type. Hence, DGs like gas turbines (GTs), micro alternators and, internal combustion engine (ICE) are classified as inertial DGs, that can be directly integrated into the conventional AC grid. Accordingly, the inverter type of DGs requires power electronic interface for grid connection and consists of a power generation system such as PV, WT and fuel cells (FCs) [10]–[14]. The ESDs constitute as an energy buffer and contribute to various aspects of power quality improvement [15]. In this front, numerous energy storage systems (ESSs) have been employed, such as flywheel energy storage (FES), supercapacitor energy storage systems (SCCESS), superconducting magnetic energy storage systems (SMES) and battery energy storage system (BESS) [16]–[18].

In addition to the integration of environmentally friendly power generation sources, RES-MGs offer lower financial responsibilities as compared to conventional centralized bulk power generation. Furthermore, the sensitivity of load towards transmission line interruptions is less severe. In short, valuable goals can be achieved, such as decrement in carbon emissions as well as lower investment costs and enhanced reliability of power supply. Nevertheless, the implementation of MGs has many regulatory and technical challenges. The technical challenges imposed, consist of power quality degradation, coordination of protective relays and dynamic stability issues [7]. Whereas, regulated government pricing,

uncompetitive electricity market and a convenient geographical requirement for RESs installment are the associated regulatory challenges. Recently, the concept of MGs has substantially gained global interest. Many kinds of academic and industrial research have been conducted to propose and implement various kinds of MG systems and their associated control strategies for deployment alongside conventional power networks. For instance, the MG project of China [19], the MG project of Venezuela [20], the MG research in Federal University of Rio de Janeiro in Brazil [21], and numerous projects in the United States [22].

In accordance with the literature, MGs' control strategies are broadly categorized into centralized and decentralized control architecture. In centralized control, the entire system is handled by a central control unit that shares data and information with a distribution control system through communication channels [23]. In this regard, a centralized MG control is presented in [24]. Here, the control strategy is based on the particle swarm optimization (PSO) and fuzzy logic (FL) technique for tuning the parameters of the proportional-integral (PI). The PI parametric tuning is carried according to the online measurements using FL rules. The membership functions of the FL are optimized using PSO. The authors postulated better frequency regulation (FR) in comparison to classical PI controllers and pure fuzzy-based PI controllers. In decentralized control, a dedicated controller is designed for each component of the MG system [25]. A decentralized control approach for FR and reactive power sharing (RPS) is demonstrated in [26]. In this research, power-frequency droop control is designed where the line voltage drop compensation is used to generate the frequency reference and to improve the voltage droop coefficient. Furthermore, a voltage feedback control is introduced to achieve an accurate RPS. The control strategy proposed in this study proves to flexibly and effectively operate under various DG disturbance scenarios. Similarly, a decentralized control strategy directed towards the bidirectional power converter interface that is implemented for optimal AC/DC MG integration has been studied in [27]. The main objective of the proposed control method is to achieve overall power-sharing and smooth transition between grid-connected and autonomous mode. Moreover, an ESS is utilized in the DC sub-grid to provide voltage support during the islanded mode operation. The authors verified the performance of this control strategy by real-time hardware-in-loop (HIL) tests.

ESSs are widely used to enhance the power quality and provide stability support to the MG systems in both grid-connected as well as islanded mode. Numerous prospective ESS-based control strategies have been studied in the literature [28], [29]. In [30], a PID-fuzzy controller for BESS is proposed to enhance the power quality in MGs. The efficient utilization of ESS for power quality improvement and consequently overall performance of the system are enhanced further as compared with classical PI controllers. Further, the study in [31], proposes a controller for BESS that has been designed for voltage and frequency restoration during MG

system transience. The designed controller has been tested specifically for two abnormal conditions of the MG; abrupt load changes and fault conditions. However, the performance of these two BESS-based controllers was not satisfactory in terms of response time and fluctuations magnitude. The study in [32], proposes a BESS-based control strategy to enhance the power quality in grid-tied MGs. However, this strategy is suitable only for low-level disturbances. Likewise in [33], a SCESS-based controller for MG frequency support is proposed. The controller approach based on structural singular value theory and using the DEO technique to optimize the SCESS controller gains corresponding to the MG requirements. This methodology effectively supports the MG frequency to compensate for system transience conditions. However, does not improve the MG system voltage as well. In [34], a control strategy to support and regulate the frequency and voltage of the MG during system contingencies have been proposed considering a hybrid energy storage system (HESS), which consists of BESS and SCESS along with distributed generations such as solar PV, WT, FC, and micro-generators. The author has employed a PI-based adaptive online neuro-fuzzy algorithm for optimal power allocation between the HESS components. Accordingly, other control strategies have been proposed in [35]–[39] to achieve rapid dynamic response under abnormal conditions of the MG. However, these strategies do not contribute significantly towards improving the power quality and additionally involve complex and tedious calculations.

Owing to the aforementioned analysis, this paper posits an online intelligent control approach based on hybrid differential evolution optimization and artificial neural networks (DEO-ANN). In fact, the idea is to utilize the mutual benefits of both algorithms with an optimal online tuning of two decoupled BESS-based controllers and hence improve the MG power quality. As mentioned earlier, one of the major technical concerns in MG applications is to improve the power quality of the system subjected to disturbances; particularly the problem becomes very challenging in case of unknown disturbances with significantly higher magnitude. Hence innovative hybrid intelligent control approaches are vital to cope with the problem. To the best of author's knowledge, this approach has not been proposed earlier in the literature. In this paper, the MG system under consideration consists of a synchronous generator (SG), PV, and BESS. The two decoupled BESS-based controllers have been designed to achieve optimal operation under low and high magnitude disturbances; consequently, enhancing the MG power quality by maintaining the voltage and frequency deviations at the point of common coupling (PCC) under permissible limits. The proposed controller is optimized to effectively operate under several operating conditions using the DEO technique; the collected input and output sets are used to train the ANN to perform an online tuning of the controllers' parameters. The robustness of the proposed controllers is computationally validated under random low and high magnitude disturbances. Finally, a comparative study is performed with and

without the implementation of the controllers and with the benchmark PID controller. The main advantage achieved with this controller is ease of implementation and rapid response towards voltage and frequency restoration. However, the proposed decoupled control strategy is applicable only for grid-connected MGs.

The rest of the paper is organized as follows: Section II describes the problem and the MG system configuration. In Section III, detailed mathematical modeling of the MG is presented. Section IV demonstrates the proposed decoupled control approach and problem formulation. The simulation results are discussed in section V. Finally, the conclusion is given in Section VI.

II. PROBLEM DESCRIPTION

MGs are exposed to many kinds of disturbances, for instance, the intermittency of the renewable generators, sudden loads shedding, and power system faults. Thus, appropriate control techniques are vital in order to restore the system to steady-state conditions and improve the power quality of the MG system. In this paper, two online intelligent decoupled BESS-based controllers are proposed to improve the MG power quality subjected to low and high magnitude disturbances. The detailed single line diagram (SLD) of the MG under consideration is shown in Fig. 1. The DEO technique is employed to optimize the parameters of the two controllers under a wide range of disturbances. The optimized parameters of the two controllers and the corresponding disturbances are arranged in input and output training sets to train the ANNs for optimal online tuning of the controllers' parameters. Finally, the proposed intelligent control approach is evaluated under random low and high magnitude disturbances, and its performance is compared with a benchmark controller.

III. MICROGRID SYSTEM MODEL

The mathematical representations of the MG system under consideration in this paper are provided in the following subsections.

A. SYNCHRONOUS GENERATOR

The SG can be represented mathematically by four differential equations that describe its dynamic behavior. The angular displacement, the angular frequency, the field voltage along the direct axis, and the internal voltage along the quadrature axis are described in (1), (2), (3), and (4), respectively.

$$\frac{d\delta}{dt} = \omega_0 (\omega - 1) \tag{1}$$

$$\frac{d\omega}{dt} = \frac{1}{2H} (P_m - P_e) \tag{2}$$

$$\frac{dE_{fd}}{dt} = \frac{1}{\tau_E} [\alpha_E (V_{g0} - V_g) - (E_{fd} - E_{fd0})] \tag{3}$$

$$\frac{de'_q}{dt} = \frac{1}{T'_{d0}} [E_{fd} - e'_e - (x_d - x'_d) i_{gd}] \tag{4}$$

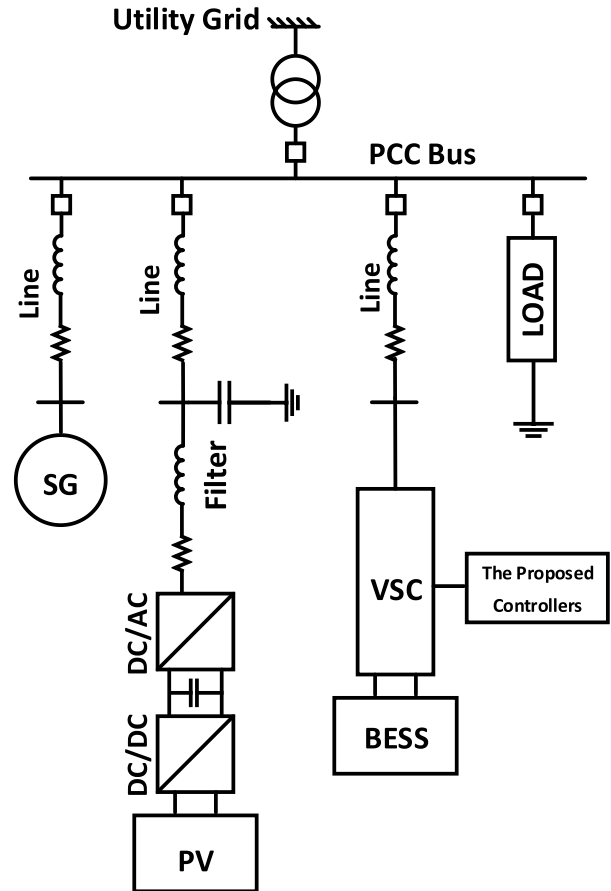


FIGURE 1. The SLD of the MG system.

B. PHOTOVOLTAIC SYSTEM

The PV cell simplified circuit model is shown in Fig. 2. It consists of a current source, a photodiode, and a series resistor.

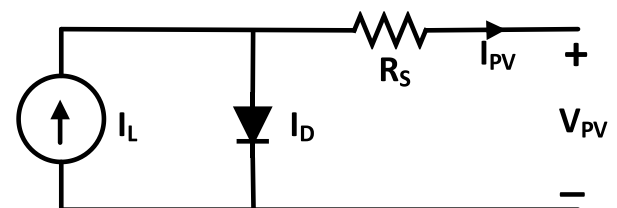


FIGURE 2. PV cell simplified circuit model.

The dynamic behavior of the PV system can be represented by eight differential equations that describe the PV cell, the DC/DC boost converter, the voltage source inverter (VSI), and the low pass (LP) filter [34]. The following subsections describe in detail the PV system model.

1) BOOST CONVERTER AND VOLTAGE SOURCE INVERTER

The DC/DC boost converter circuit model is presented in Fig. 3. As can be seen, it consists of a series inductor, an insulated-gate bipolar transistor (IGBT), a diode, and a DC

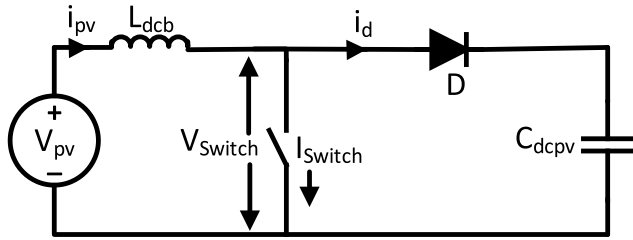


FIGURE 3. Boost converter circuit.

linking capacitor. The DC linking capacitor is mandatory to maintain constant input voltage to the VSI.

The DC/AC VSI equivalent circuit model is presented in Fig. 4. It operates in Pulse-width modulation (PWM) mode with two controlling parameters, which are the modulation index and the phase angle.

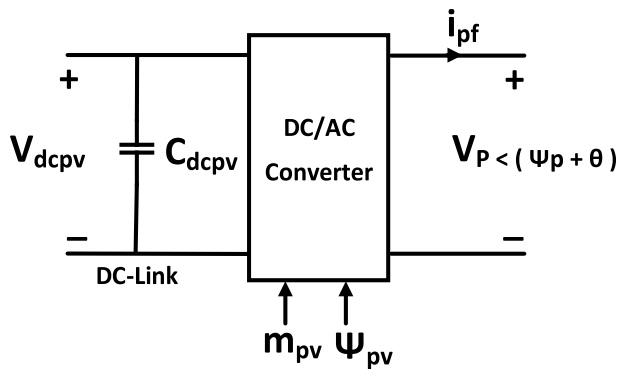


FIGURE 4. The VSI circuit model.

The mathematical expressions in (5), (6), (7), and (8) represent the PV cell output current, the DC linking capacitor voltage, the output current of the VSI in the d-axis, and the output current of the VSI in q-axis, respectively.

$$\frac{di_{pv}}{dt} = \frac{1}{L_b} [V_{pv} - (1 - d_{pv}) V_{dcpv}] \quad (5)$$

$$\frac{dV_{dcpv}}{dt} = \frac{1}{C_{dcpv}} [(1 - d_{pv}) i_{pv} - m_{pv} i_{pfd} \cos(\psi_{pv} + \theta)] \quad (6)$$

$$\begin{aligned} \frac{di_{pfd}}{dt} = & \frac{-\omega_0 R_{pf}}{L_{pf}} i_{pfd} + \omega_0 \omega i_{pfq} + \frac{\omega_0 m_{pv} V_{dcpv} \cos(\psi_{pv} + \theta)}{L_{pf}} \\ & - \frac{\omega_0 V_{cpd}}{L_{pf}} - \omega_0 R_{pdr} (i_{pfd} - i_{pd}) \end{aligned} \quad (7)$$

$$\begin{aligned} \frac{di_{pdq}}{dt} = & \frac{-\omega_0 R_{pf}}{L_{pf}} i_{pfq} + \omega_0 \omega i_{pfd} + \frac{\omega_0 m_{pv} V_{dcpv} \sin(\psi_{pv} + \theta)}{L_{pf}} \\ & - \frac{\omega_0 V_{cpq}}{L_{pf}} - \omega_0 R_{pdr} (i_{pfq} - i_{pq}) \end{aligned} \quad (8)$$

2) LOW PASS FILTER AND TRANSMISSION LINE

The LP filter circuit and the coupling transmission line model are shown in Fig. 5.

The LP filter capacitor voltage in d-axis, the LP filter capacitor voltage in q-axis, the LP filter output current in

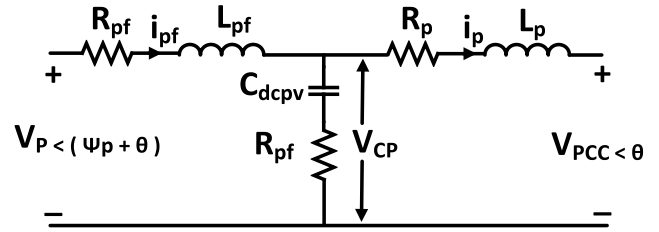


FIGURE 5. The LP filter and transmission line model.

d-axis, and the LP filter output current in q-axis are expressed in the following mathematical expressions (9), (10), (11) and (12), respectively.

$$\frac{dV_{cpd}}{dt} = \frac{1}{C_{pf}} (i_{pfd} - i_{pd}) + \omega_0 \omega V_{cpq} \quad (9)$$

$$\frac{dV_{cpq}}{dt} = \frac{1}{C_{pf}} (i_{pfq} - i_{pq}) + \omega_0 \omega V_{cpd} \quad (10)$$

$$\begin{aligned} \frac{di_{pd}}{dt} = & \frac{-\omega_0 R_p}{L_p} i_{pd} + \omega_0 \omega i_{pq} \\ & + \frac{\omega_0}{L_p} (V_{cpd} - V_{sd}) + \omega_0 R_{pdr} (i_{pfd} - i_{pd}) \end{aligned} \quad (11)$$

$$\begin{aligned} \frac{di_{pq}}{dt} = & \frac{-\omega_0 R_p}{L_p} i_{pq} + \omega_0 \omega i_{pd} \\ & + \frac{\omega_0}{L_p} (V_{cpq} - V_{sq}) + \omega_0 R_{pdr} (i_{pfq} - i_{pq}) \end{aligned} \quad (12)$$

3) BATTERY ENERGY STORAGE SYSTEM

The BESS circuit model is shown in Fig. 6. It consists of a DC voltage source, a series resistor, and a DC linking capacitor connected to the PCC bus through VSC. The BESS can be modeled mathematically by three differential equations that represent the DC linking capacitor voltage (13), the BESS output current in d-axis (14), and the BESS output current in the q-axis (15) [34].

$$\frac{dV_{dcs}}{dt} = \frac{m_B}{C_{dcs}} (i_{stq} \cos(\psi_B) + i_{std} \sin(\psi_B)) + \frac{V_B - V_{dcs}}{R_B C_{dcs}} \quad (13)$$

$$\begin{aligned} \frac{di_{std}}{dt} = & \frac{-\omega_0 R_{st}}{L_{st}} i_{std} + \frac{\omega}{\omega_0} i_{stq} \\ & + \frac{\omega_0}{L_{st}} (m_B V_{dcs} \cos(\theta + \psi_B) - V_{sd}) \end{aligned} \quad (14)$$

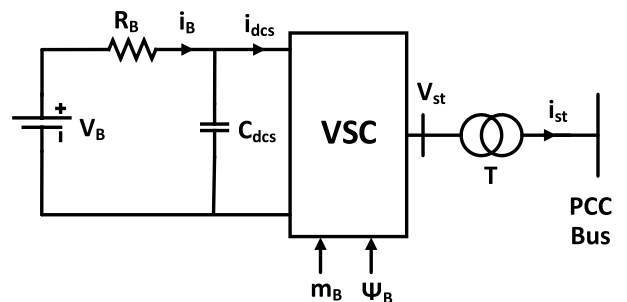


FIGURE 6. The BESS circuit model.

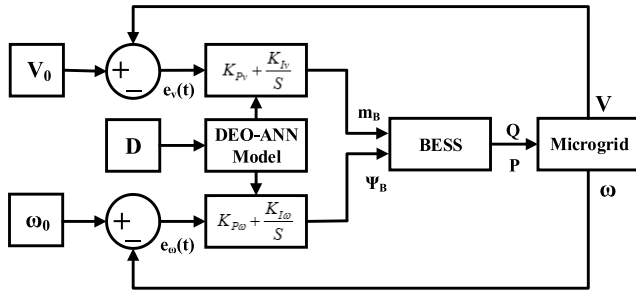


FIGURE 7. The proposed control approach diagram.

$$\frac{di_{stq}}{dt} = \frac{-\omega_0 R_{st}}{L_{st}} i_{stq} + \frac{\omega}{\omega_0} i_{std} + \frac{\omega_0}{L_{st}} (m_B V_{dcs} \sin(\theta + \psi_B) - V_{sq}) \quad (15)$$

IV. THE PROPOSED APPROACH

Two intelligent decoupled BESS-based PI controllers are proposed in this paper to improve the MG power quality by restoring the MG voltage and frequency to normal operating conditions following a disturbance. The two intelligent controllers are designed based on hybrid DEO and ANNs techniques. The MG voltage and frequency are decoupled by independently controlling the BESS output active and reactive power. Fig. 7 shows the proposed control approach diagram, where the phase angle and the modulation index of the VSC are controlled separately by two BESS-based PI controllers. The phase angle controls the BESS active power needed to be supplied or absorbed. Whereas, the modulation index controls the amount of reactive power required to be supplied or absorbed by the BESS. As per the expressions (16) and (17), the voltage and frequency of the MG are compared with reference values at first. Then, the mismatches, which represent errors, are entered into the two PI controllers in order to be minimized. After that, the developed hybrid approach tunes the controllers with the optimal parameters based on the disturbance level.

$$m_B = K_{Pv} e_v(t) + K_{Iv} \int_0^t e_v(t) dt \quad (16)$$

$$\psi_B = K_{P\omega} e_\omega(t) + K_{I\omega} \int_0^t e_\omega(t) dt \quad (17)$$

Consequently, the BESS supplies or absorbs the needed amount of active and reactive power, based on the stability requirements of the MG system. The active power will enhance MG frequency by damping the system oscillations. Whereas, the reactive power will improve the MG PCC bus voltage profile. As a result, the overall power quality of the system is improved.

Searching the optimal controllers' parameters can be formulated as two optimization problems, where the two objective functions are the minimization of the voltage integral squared-error (ISE) (18) and the frequency ISE (19).

$$\text{Min} \int_0^t e_v(t)^2 dt = \int_0^t (\Delta V)^2 dt = \int_0^t (V_0 - V)^2 dt \quad (18)$$

$$\text{Min} \int_0^t e_\omega(t)^2 dt = \int_0^t (\Delta \omega)^2 dt = \int_0^t (\omega_0 - \omega)^2 dt \quad (19)$$

The above two objective functions are subjected to the following constraints:

- The permissive operation limits of MG frequency and PCC bus voltage in per-unit values.

$$0.999 \leq \text{Frequency} \leq 1.001$$

$$0.95 \leq \text{Voltage} \leq 1.05$$

- The two PI controllers' parameters limits and maximum overshoot response.

$$30 \leq K_{P\omega}, K_{Pv} \leq 150$$

$$50 \leq K_{I\omega}, K_{Iv} \leq 250$$

$$\text{Overshoot} \leq 10\%$$

As known, there is a tradeoff between stabilization time and overshoot in PI controller response such that the proportional parameters ($K_{P\omega}$ and K_{Pv}) affect the overshoot, and the integral parameter ($K_{I\omega}$ and K_{Iv}) affect the stabilization time [40]. Hence, predefined ranges for the controller parameters are required to ensure that the response of the system will not violate the prescribed operation limits for the MG frequency and voltage. The limits for the controllers' parameters have been determined by trial and error during the simulation and observing the optimal parameter values that do not adversely jeopardize the response of the system.

The proposed hybrid optimization approach is based on the DEO and ANN techniques. The DEO is a powerful stochastic optimization technique that is distinguished by its simplicity and robustness. Besides, it can solve complex nonlinear problems and converge fast to the optimal solution. The DEO is a population-based optimization algorithm which operates through similar computational steps as employed by a standard evolutionary algorithm (EA). The EA uses iterative progress, such as growth or development in a population that is selected in a guided random search using parallel processing to achieve the desired objective. Contrasting other EA methods, the DEO is very immune against falling into local optimums and has less setting parameters [41]–[43].

The setting parameters of the DEO technique are presented in Table 1. The optimal generation number and population size are determined by experience and by trial and error during the simulation. Fig. 8 and Fig. 9 show the convergence of the two objective functions (18) and (19) over 100 generations for different levels of disturbances from 1 p.u to 4 p.u. It can be observed from the two figures that the selected setting parameters for the DEO algorithm ensure that the optimal solution is reached for both objective functions.

The flow chart in Fig. 10 describes in detail the DEO technique. After Applying a disturbance, the DEO algorithm starts first with an initial population of 50 solutions (i.e., controllers' parameters) that have been randomly initialized. Then, the objective functions are calculated as per the expressions (18) and (19) for all the randomly initialized controllers' parameters. The best parameters that give the

TABLE 1. The DEO algorithm parameters.

Parameter description	Value
Generation number	100
Population size	50
Mutation factor	0.5
Crossover factor	0.7

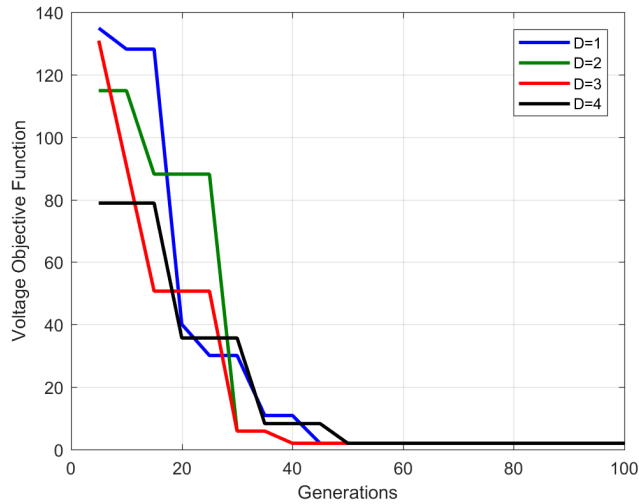


FIGURE 8. The convergence of the voltage objective function to the optimal solution.

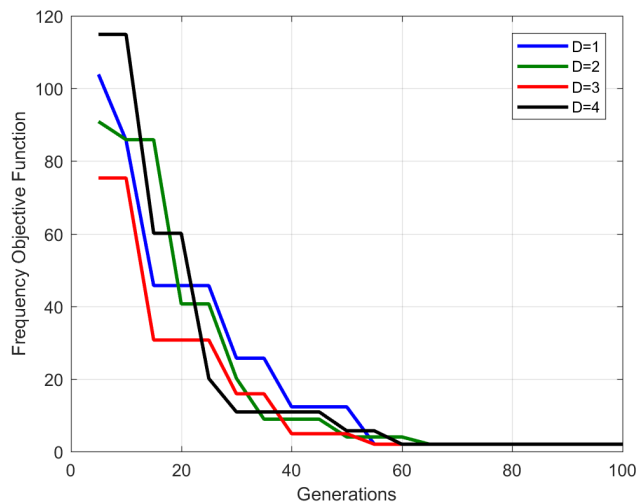


FIGURE 9. The convergence of the frequency objective function to the optimal solution.

minimum voltage ISE and frequency ISE values are searched and saved. Each population undergoes a mutation and crossover process in order to get new generations, and the best solutions are searched again and saved. In doing so, the algorithm checks the stopping criteria, which is reaching up to 100 generations that is the maximum generation number (MAX_GEN_NUM) in this paper. Finally, when the stopping

criteria is reached, the algorithm stops and gives the optimal parameters for the two decoupled PI controllers.

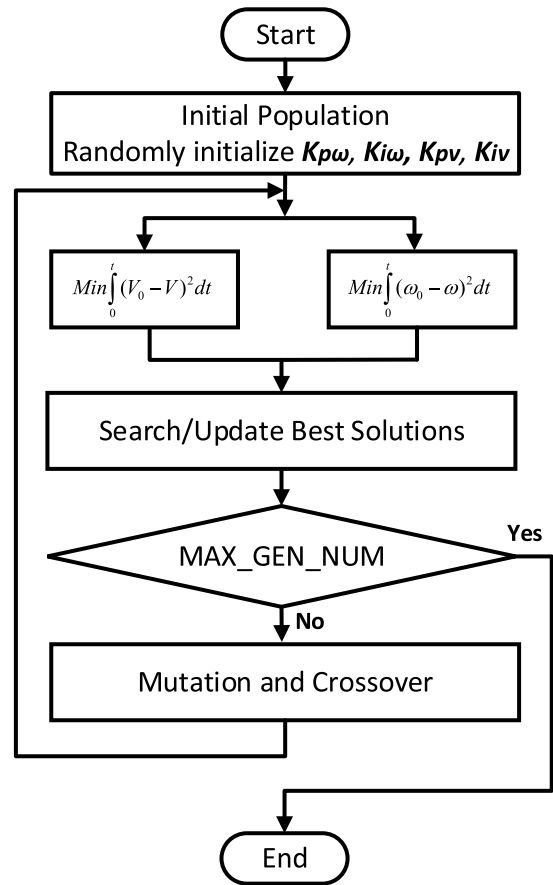


FIGURE 10. The DEO algorithm.

The proposed hybrid DEO and ANN approach is described in Algorithm 1. As can be seen, the algorithm starts with applying a disturbance level ranging from 0.1 p.u to 4 p.u. in steps of 0.013 p.u to the MG system. In this paper, 300 levels of disturbances have been applied. These disturbances simulate sudden changes in the input mechanical torque of the SG. After that, the algorithm runs the DEO to find optimum controllers' parameters of the two decoupled BESS-based PI controllers for each disturbance level as described in Fig. 10. Then, the obtained optimal parameters, as well as the disturbances, are used to develop and train the ANN, as shown in Fig. 11. The input to the ANN is the disturbance levels, and the output of the ANN is the optimal controllers' parameters. The developed network consists of one input layer, one hidden layer with 300 neurons, and one output layer with four neurons. This kind of ANNs called multi-layer feed-forward neural network (MLFFNN), which is the most popular structure of ANNs. In this paper, the constructive technique is used to construct the hidden layer neurons of the developed ANN. The activation functions for the hidden neurons and the output neurons were the commonly used functions, i.e. the tangent sigmoid and the linear function, respectively. The backpropagation training

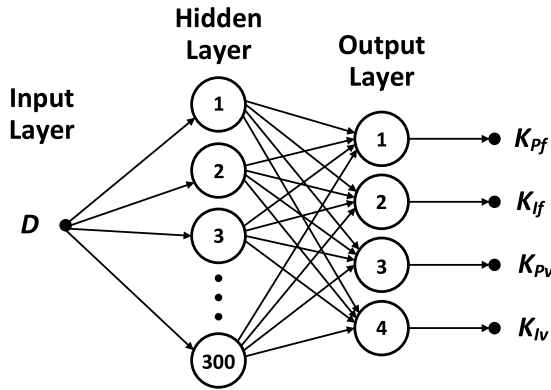


FIGURE 11. The developed ANN.

function “trainlm” in the ANN toolbox in MATLAB has been implemented to train the ANN for each operating condition. This training function compares the obtained controller outputs with the targeted outputs. Then, the error signal is propagated back to adjust the ANN weighting matrices and biases, according to Levenberg-Marquardt optimization [44]. The training process continues until getting the optimal ANN that can identify the optimal controllers’ parameters for any disturbance level within the training range.

Algorithm 1 The Proposed Hybrid DEO and ANN Technique

Start

Applying a disturbance level (D)

$D = 0.1$

while $i \leq 300$ **do**

• **Saving the disturbance level**

$D \rightarrow Input_Vector$

• **Running the DEO algorithm as per Fig. 10**

Initialization of $K_{P\omega}, K_{Pv}, K_{I\omega}, K_{Iv}$

Calculation of objective functions (18) and (19)

Mutation and crossover

Getting the optimal $K_{P\omega}, K_{Pv}, K_{I\omega}, K_{Iv}$

• **Saving the optimal controllers’ parameters**

$K_{P\omega}, K_{Pv}, K_{I\omega}, K_{Iv} \rightarrow Output_Vectors$

$D = D + 0.013$ **end while**

• **Developing the ANN as per Fig. 11**

Training the ANN with:

$Input_Vector$ & $Output_Vectors$

Generating the training performance curves

Saving the trained ANN.

• **Testing the hybrid DEO and ANN technique**

Applying a new level of Disturbance

Plot MG voltage and frequency response curves

End

Fig. 12 and Fig. 13 show the training data fit and performance curves of the developed artificial neural network, respectively. As can be seen in Fig. 12 the training data (in black circles) are perfectly fit in the regression line (in blue)

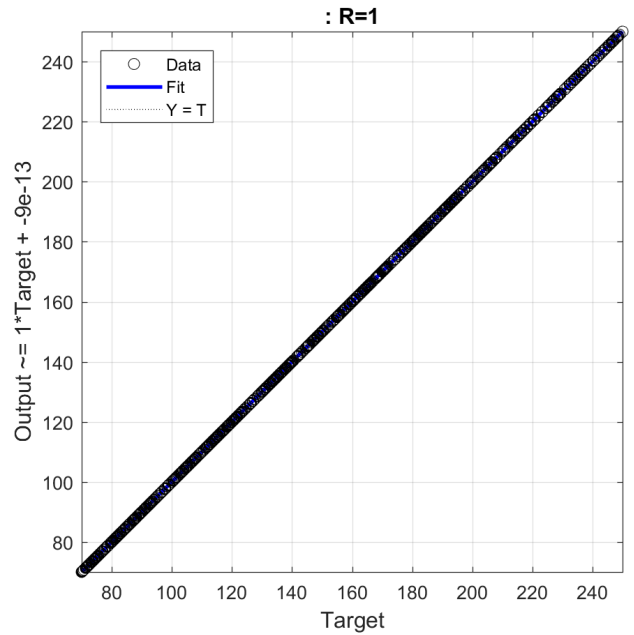


FIGURE 12. The ANN training data fit.

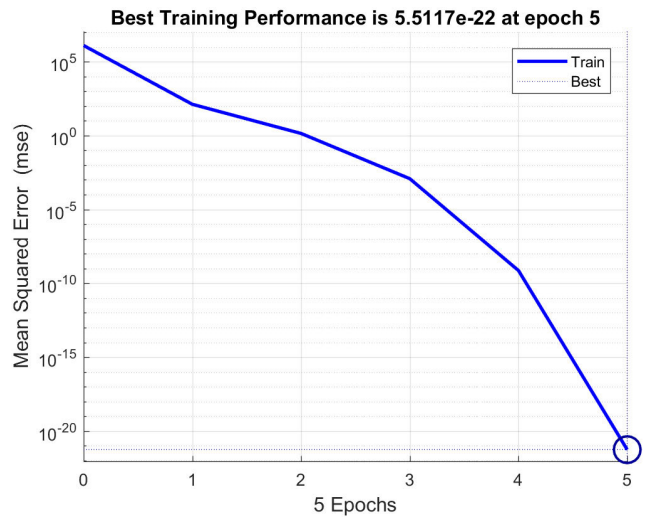


FIGURE 13. The ANN training performance curve.

with correlation factor $R = 1$. Additionally, it can be observed from Fig. 13 that the best training performance found to be at Epoch number 5 with MSE converges to zero, which indicates that the developed ANN is well trained.

V. RESULTS AND DISCUSSIONS

In order to verify the effectiveness and robustness of the proposed control approach, two randomly generated low-level and high-level disturbances between (0.1 p.u) and (4 p.u) have been applied to the MG system. The dynamic responses of the system with and without the action of proposed controllers along with a performance comparison with the well-known benchmark PID controller are provided in the following

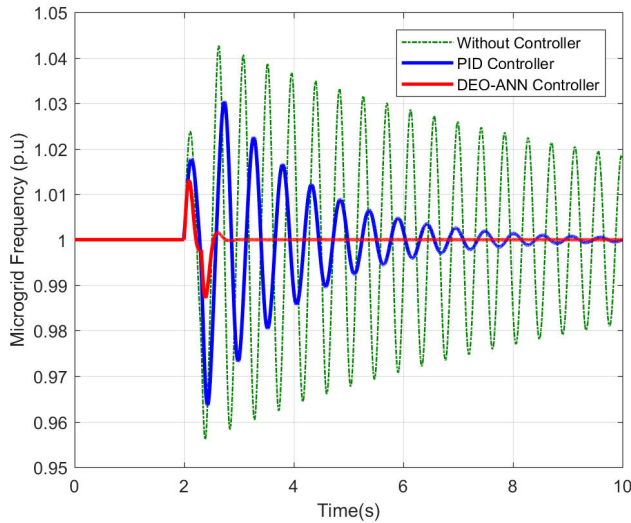


FIGURE 14. The MG frequency (in p.u).

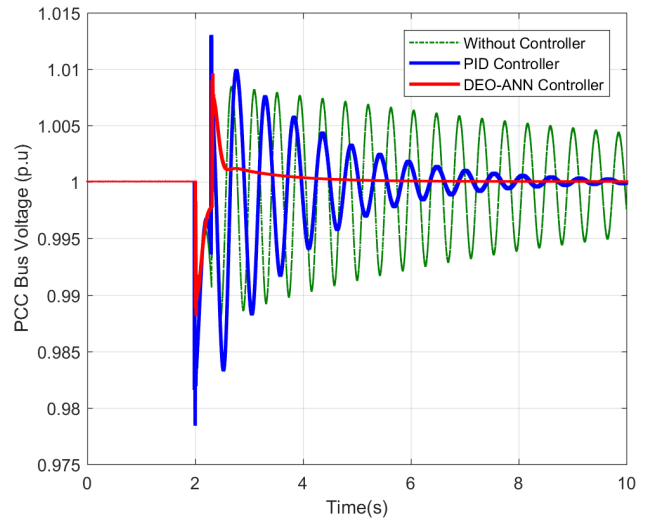


FIGURE 15. The MG PCC bus voltage (in p.u).

subsections. In fact, the PID controller is widely used as a benchmark controller, and many papers in the literature compare the performance of their proposed controllers with the performance of the classical PID controller [30]–[34].

A. AT LOW-LEVEL DISTURBANCES

A random low magnitude disturbance has been generated (0.512 p.u) and applied to the MG system. The proposed two decoupled controllers have generated the optimal controllers' parameters, as shown in Table 2.

TABLE 2. The optimal controllers' parameters at a low-level disturbance.

Controller parameter	Value
$K_{P\omega}$	73.28
$K_{I\omega}$	146.39
K_{Pv}	61.74
K_{Iv}	121.58

Fig. 14 and Fig. 15 show the dynamic responses of the MG system frequency and voltage with the action of the proposed DEO-ANN decoupled controllers (in red), the PID controller (in blue), and without controller actions (in dotted green). It can be observed that in the absence of the control action, the oscillations in the MG system frequency and voltage continue for a more extended period of time. However, with the action of the proposed DEO-ANN controllers, the oscillations are damped quickly and returned to the steady-state condition in less than 2 seconds. Furthermore, the proposed DEO-ANN controllers performed better than the PID controller in terms of stabilization time and overshoot, as can be seen in the following two figures.

The BESS mitigates the oscillations of the MG system quantities by injecting or absorbing the required amount of

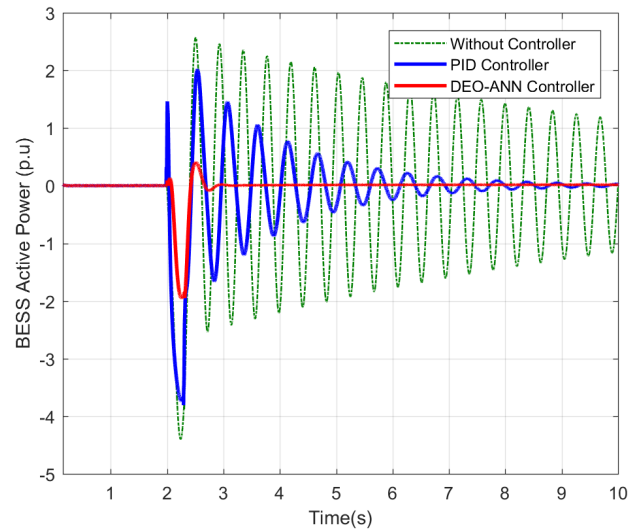


FIGURE 16. The BESS injected active power (in p.u).

active and reactive power properly. The active power contributes to frequency stability, and the reactive power recovers the MG voltage to steady-state conditions. Thus, the MG system's overall power quality is improved. Fig. 16 and Fig. 17 show the BESS dynamic performance subjected to the applied disturbance level with and without the action of the proposed DEO-ANN controllers as compared with the PID controller response. As can be seen, without appropriate control, the BESS active and reactive power fluctuate for an extended period of time. Whereas, with the presence of the proposed DEO-ANN controllers, the BESS restored the system to normal operating conditions in about 1.5 seconds.

Moreover, the proposed DEO-ANN controllers achieved superior performance over the PID controller in both stabilization time and overshoot. Therefore, the effectiveness

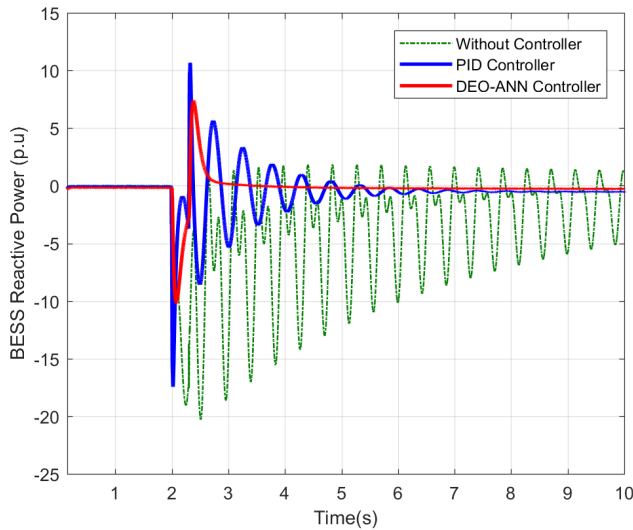


FIGURE 17. The BESS injected reactive power (in p.u).

of the proposed control approach has been verified under low-level disturbances.

B. AT HIGH-LEVEL DISTURBANCES

In order to verify the robustness of the proposed two decoupled controllers, a random high magnitude disturbance has been generated (3.287 p.u) and applied to the MG system. The optimal parameters generated by the two proposed controllers are shown in Table 3.

TABLE 3. The optimal controllers’ parameters at a high-level disturbance.

Controller parameter	Value
$K_{P\omega}$	91.13
$K_{I\omega}$	173.22
K_{Pv}	78.06
K_{Iv}	156.41

Fig. 18 and Fig. 19 show the variations in the MG system frequency and voltage, respectively. It can be observed from these two figures that without a control action, the MG system frequency and voltage oscillate for more than 10 seconds. However, the proposed DEO-ANN controllers restored the system to the steady-state condition in less than 2 seconds. Additionally, the proposed DEO-ANN controllers achieved less stabilization time and response overshoot as compared with the PID controller.

In order to show the superiority of the proposed control approach at critical disturbances, the proposed controller has been compared with the PID controller in terms of the following performance indices; Integral of Absolute Error (IAE), Integral of Squared Error (ISE), Integral of Time multiplied Squared Error (ITSE), Integral of Time multiplied Absolute

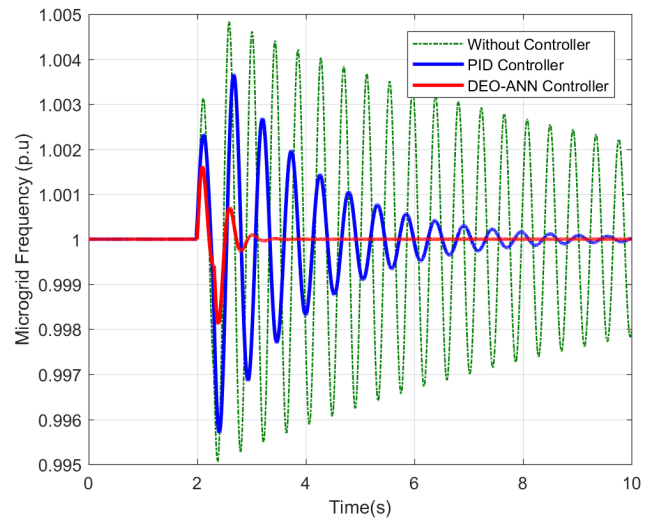


FIGURE 18. The MG frequency (in p.u).

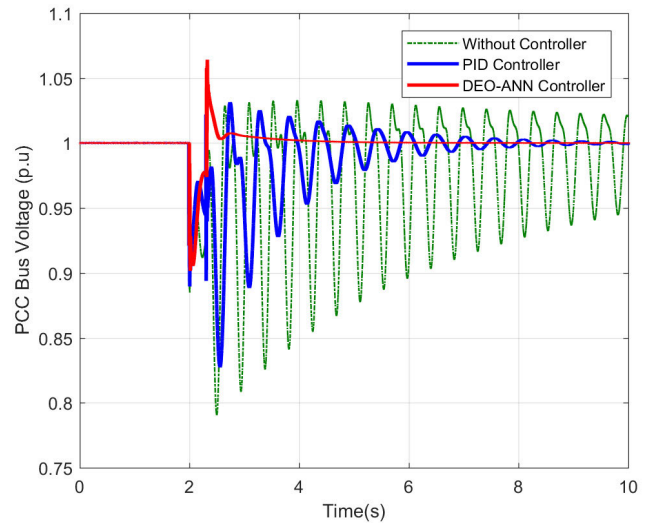


FIGURE 19. The MG PCC bus voltage (in p.u).

Error (ITAE), overshoot, and settling time. These indices are the most performance measures that are considered in control design [45]. Table 4 and Table 5 show a quantitative comparison between the performance of the proposed DEO-ANN controller and the PID controller for the MG frequency and voltage response. As can be seen, at critical disturbances, the proposed controllers surpassed the PID controller in all the performance measures.

Fig. 20 and Fig. 21 show the BESS dynamic performance subjected to the applied high magnitude disturbance in the presence and absence of the controllers’ actions. It can be noticed that the uncontrolled case leads to continuous oscillations in the BESS active and reactive power. However, the dynamic responses with the proposed DEO-ANN controllers are improved, and the BESS active and reactive power restored to normal operating conditions in less than 2 seconds.

TABLE 4. Performance indices comparison between the two controllers for the microgrid frequency response.

Performance Index	The DEO-ANN Controller	The PID Controller
IAS	6.76×10^{-4}	1.90×10^{-2}
ISE	9.66×10^{-4}	0.0242
ITSE	2.16×10^{-7}	5.31×10^{-4}
ITAE	1.55×10^{-6}	6.24×10^{-3}
Overshoot (%)	1.55	3.5
Settling time (s)	1.12	5.34

TABLE 5. Performance indices comparison between the two controllers for the microgrid voltage response.

Performance Index	The DEO-ANN Controller	The PID Controller
IAS	1.6×10^{-3}	0.073
ISE	2.13×10^{-4}	6.74×10^{-2}
ITSE	5.55×10^{-6}	2.37×10^{-3}
ITAE	4.87×10^{-6}	7.06×10^{-2}
Overshoot (%)	1.25	2.21
Settling time (s)	1.96	7.11

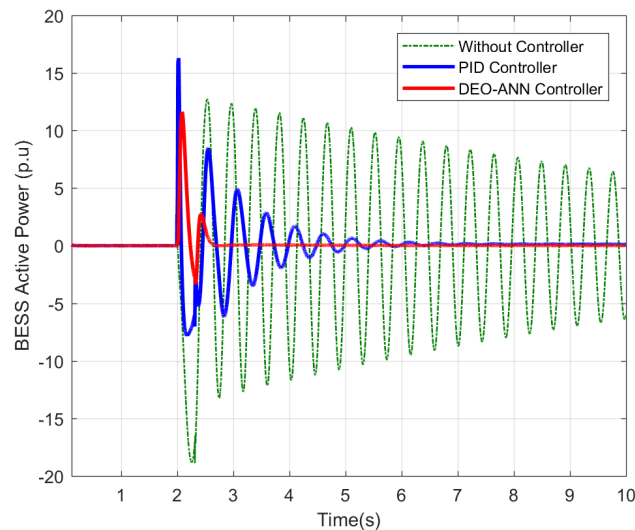


FIGURE 20. The BESS injected active power (in p.u.).

Furthermore, the proposed DEO-ANN controllers have also achieved better performance at higher magnitude disturbances as compared with the PID controller in both stabilization time and overshoot. Hence the robustness of the proposed control approach has been verified under high magnitude disturbances.

It can be observed from the simulation results that the proposed DEO-ANN controllers have successfully managed

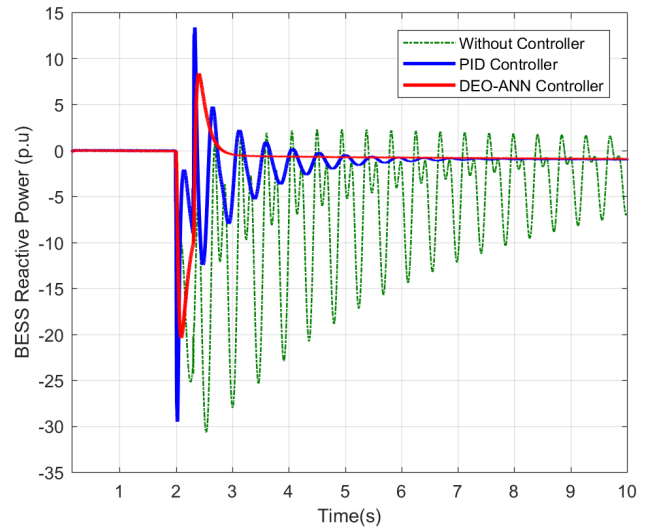


FIGURE 21. The BESS injected reactive power (in p.u.).

the active and reactive power flow from and to the BESS in order to improve the MG power quality. Furthermore, the proposed DEO-ANN controllers performed better in terms of all the above performance indices when compared with the benchmark PID controller. Moreover, the proposed DEO-ANN controllers in all the given disturbance scenarios were capable of keeping both the percentage of overshoot along with stabilization time to the minimum level without violating the prescribed constraints. Hence, the simulation results have proven the effectiveness and robustness of the proposed control approach.

VI. CONCLUSION

An intelligent decoupled BESS-based control approach has been proposed in this paper to improve the MG power quality subjected to higher magnitude disturbances; particularly, frequency and voltage restoration to steady-state conditions are targeted. The overall control approach is based on the combination of two key techniques, DEO and ANN, hence making a hybrid control system actually to utilize the complementary benefits of both techniques. The MG frequency and PCC bus voltage have been maintained within prescribed operating limits during normal and abnormal conditions. The parameters of the two BESS-based controllers have been optimized using the DEO technique under different levels of disturbances. Consequently, the optimized controllers' parameters and the corresponding disturbances are arranged in input and output sets in order to train the ANN for optimal online tuning of the two BESS-based controllers. Finally, the proposed intelligent control approach has been evaluated under random low and high magnitude disturbances in order to verify its performance as compared with the benchmark PID controller. The simulation results proved the effectiveness and robustness of the proposed control approach. Future work will be on extending the proposed control strategy to be applicable for autonomous microgrids.

ACKNOWLEDGMENT

The authors would like to thank Mr. Mohammed Ashraf Ali for his assistance in finalizing the MG model parameters. Also, this work was supported in part by the King Abdullah City for Atomic and Renewable Energy (K.A. CARE).

REFERENCES

- [1] T. S. Ustun, C. Ozansoy, and A. Zayegh, "Recent developments in microgrids and example cases around the world—A review," *Renew. Sustain. Energy Rev.*, vol. 15, no. 8, pp. 4030–4041, Oct. 2011.
- [2] N. W. A. Lidula and A. D. Rajapakse, "Microgrids research: A review of experimental microgrids and test systems," *Renew. Sustain. Energy Rev.*, vol. 15, no. 1, pp. 186–202, 2011.
- [3] S. M. Kaviri, M. Pahlevani, P. Jain, and A. Bakhshai, "A review of AC microgrid control methods," in *Proc. 8th Int. Symp. Power Electron. Distrib. Gener. Syst. (PEDG)*, Apr. 2017, pp. 1–8.
- [4] M. Khalid, U. Akram, and S. Shafiq, "Optimal planning of multiple distributed generating units and storage in active distribution networks," *IEEE Access*, vol. 6, pp. 55234–55244, 2018.
- [5] J. Huang, C. Jiang, and R. Xu, "A review on distributed energy resources and MicroGrid," *Renew. Sustain. Energy Rev.*, vol. 12, no. 9, pp. 2472–2483, 2008.
- [6] M. S. Mahmoud, S. A. Hussain, and M. A. Abido, "Modeling and control of microgrid: An overview," *J. Franklin Inst.*, vol. 351, no. 5, pp. 2822–2859, May 2014.
- [7] P. Basak, S. Chowdhury, S. H. N. Dey, and S. P. Chowdhury, "A literature review on integration of distributed energy resources in the perspective of control, protection and stability of microgrid," *Renew. Sustain. Energy Rev.*, vol. 16, no. 8, pp. 5545–5556, Aug. 2012.
- [8] T. C. Green and M. Prodanovic, "Control of inverter-based micro-grids," *Electr. Power Syst. Res.*, vol. 77, no. 9, pp. 1204–1213, Jul. 2007.
- [9] M. Kumar and B. Tyagi, "A state of art review of microgrid control and integration aspects," in *Proc. 7th India Int. Conf. Power Electron. (IICPE)*, Patiala, India, Nov. 2016, pp. 1–6.
- [10] I. Vechiu, O. Curea, A. Llaría, and H. Camblong, "Control of power converters for microgrids," *Int. J. Comput. Math. Electr. Electron. Eng.*, vol. 30, no. 1, pp. 300–309, Jan. 2011.
- [11] M. N. Marwali, J.-W. Jung, and A. Keyhani, "Control of distributed generation systems—Part II: Load sharing control," *IEEE Trans. Power Electron.*, vol. 19, no. 6, pp. 1551–1561, Nov. 2004.
- [12] J. M. Carrasco, L. G. Franquelo, J. T. Bialasiewicz, E. Galvan, R. C. Portilloiguisado, M. A. M. Prats, M. A. M. Prats, J. I. Leon, and N. Moreno-Alfonso, "Power-electronic systems for the grid integration of renewable energy sources: A survey," *IEEE Trans. Ind. Electron.*, vol. 53, no. 4, pp. 1002–1016, Jun. 2006.
- [13] F. Blaabjerg, Z. Chen, and S. B. Kjaer, "Power electronics as efficient interface in dispersed power generation systems," *IEEE Trans. Power Electron.*, vol. 19, no. 5, pp. 1184–1194, Sep. 2004.
- [14] F. Katiraei, M. R. Iravani, and P. W. Lehn, "Micro-grid autonomous operation during and subsequent to islanding process," *IEEE Trans. Power Del.*, vol. 20, no. 1, pp. 248–257, Jan. 2005.
- [15] A. G. Tsikalakis and N. D. Hatziargyriou, "Centralized control for optimizing microgrids operation," in *Proc. Power Energy Soc. Gen. Meeting*, Jul. 2011, pp. 1–8.
- [16] R. Zamora and A. K. Srivastava, "Controls for microgrids with storage: Review, challenges, and research needs," *Renew. Sustain. Energy Rev.*, vol. 14, no. 7, pp. 2009–2018, Sep. 2010.
- [17] P. F. Ribeiro, B. K. Johnson, M. L. Crow, A. Arsoy, and Y. Liu, "Energy storage systems for advanced power applications," *Proc. IEEE*, vol. 89, no. 12, pp. 1744–1756, Dec. 2001.
- [18] U. Akram and M. Khalid, "A coordinated frequency regulation framework based on hybrid battery-ultracapacitor energy storage technologies," *IEEE Access*, vol. 6, pp. 7310–7320, 2018.
- [19] B. Zhao, J. Chen, L. Zhang, X. Zhang, R. Qin, and X. Lin, "Three representative island microgrids in the East China Sea: Key technologies and experiences," *Renew. Sustain. Energy Rev.*, vol. 96, pp. 262–274, 2018.
- [20] A. López-González, B. Domenech, and L. Ferrer-Martí, "Sustainability and design assessment of rural hybrid microgrids in venezuela," *Energy*, vol. 159, pp. 229–242, Sep. 2018.
- [21] M. H. Bellido, L. P. Rosa, A. O. Pereira, D. M. Falcão, and S. K. Ribeiro, "Barriers, challenges and opportunities for microgrid implementation: The case of federal university of Rio de Janeiro," *J. Cleaner Prod.*, vol. 188, pp. 203–216, Jul. 2018.
- [22] W. Feng, M. Jin, X. Liu, Y. Bao, C. Marnay, C. Yao, and J. Yu, "A review of microgrid development in the united states—A decade of progress on policies, demonstrations, controls, and software tools," *Appl. Energy*, vol. 228, pp. 1656–1668, Oct. 2018.
- [23] S. Parhizi, H. Lotfi, A. Khodaei, and S. Bahramirad, "State of the art in research on microgrids: A review," *IEEE Access*, vol. 3, pp. 890–925, 2015.
- [24] H. Bevrani, F. Habibi, P. Babahajyani, M. Watanabe, and Y. Mitani, "Intelligent frequency control in an AC microgrid: Online PSO-based fuzzy tuning approach," *IEEE Trans. Smart Grid*, vol. 3, no. 4, pp. 1935–1944, Dec. 2012.
- [25] K. S. Rajesh, S. S. Dash, R. Rajagopal, and R. Sridhar, "A review on control of ac microgrid," *Renew. Sustain. Energy Rev.*, vol. 71, no. 1, pp. 814–819, 2017.
- [26] Z. Zhang, C. Dou, D. Yue, B. Zhang, and W. Luo, "A decentralized control method for frequency restoration and accurate reactive power sharing in islanded microgrids," *J. Franklin Inst.*, vol. 355, no. 17, pp. 8874–8890, 2018.
- [27] P. Yang, Y. Xia, M. Yu, W. Wei, and Y. Peng, "A decentralized coordination control method for parallel bidirectional power converters in a hybrid AC-DC microgrid," *IEEE Trans. Ind. Electron.*, vol. 65, no. 8, pp. 6217–6228, Aug. 2018.
- [28] M. Faisal, M. Hannan, P. J. Ker, A. Hussain, M. Mansur, and F. Blaabjerg, "Review of energy storage system technologies in microgrid applications: Issues and challenges," *IEEE Access*, vol. 6, pp. 35143–35164, 2018.
- [29] U. Akram, M. Khalid, and S. Shafiq, "An innovative hybrid wind-solar and battery-supercapacitor microgrid system-development and optimization," *IEEE Access*, vol. 5, pp. 25897–25912, 2017.
- [30] G. Parise, L. Martirano, M. Kermani, and M. Kermani, "Designing a power control strategy in a microgrid using PID / fuzzy controller based on battery energy storage," in *Proc. Int. Conf. Environ. Elect. Eng. Ind. Commercial Power Syst. Eur. (EEEIC / I&CPS Eur.)*, Milan, Italy, Jun. 2017, pp. 1–5.
- [31] M. Kermani, "Transient voltage and frequency stability of an isolated microgrid based on energy storage systems," in *Proc. 16th Int. Conf. Environ. Electr. Eng. (EEEIC)*, Florence, Italy, Jun. 2016, pp. 1–5.
- [32] J. Alshehri, M. Khalid, and A. Alzahrani, "An intelligent battery energy storage-based controller for power quality improvement in microgrids," *Energies*, vol. 12, no. 11, p. 2112, Jun. 2019.
- [33] H. Li, X. Wang, and J. Xiao, "Differential evolution-based load frequency robust control for micro-grids with energy storage systems," *Energies*, vol. 11, no. 7, p. 1686, Jun. 2018.
- [34] M. A. Ali, "Control of a microgrid through energy storage devices using evolutionary and neuro-fuzzy methods," M.S. thesis, Dept. Elect. Eng., King Fahd Univ. Petroleum Minerals, Dhahran, Saudi Arabia, 2013.
- [35] C. Fu and W. Tan, "Decentralised load frequency control for power systems with communication delays via active disturbance rejection," *IET Gener., Transmiss. Distrib.*, vol. 12, no. 6, pp. 1397–1403, Mar. 2018.
- [36] M. Ma, C. Zhang, X. Liu, and H. Chen, "Distributed model predictive load frequency control of the multi-area power system after deregulation," *IEEE Trans. Ind. Electron.*, vol. 64, no. 6, pp. 5129–5139, Jun. 2017.
- [37] R. Shankar, K. Chatterjee, and R. Bhushan, "Impact of energy storage system on load frequency control for diverse sources of interconnected power system in deregulated power environment," *Int. J. Electr. Power Energy Syst.*, vol. 79, pp. 11–26, Jul. 2016.
- [38] C. Mu, Y. Tang, and H. He, "Improved sliding mode design for load frequency control of power system integrated an adaptive learning strategy," *IEEE Trans. Ind. Electron.*, vol. 64, no. 8, pp. 6742–6751, Aug. 2017.
- [39] G. Rinaldi, M. Cucuzzella, and A. Ferrara, "Third order sliding mode observer-based approach for distributed optimal load frequency control," *IEEE Control Syst. Lett.*, vol. 1, no. 2, pp. 215–220, Oct. 2017.
- [40] K. J. Åström and T. Hägglund, "Revisiting the Ziegler–Nichols step response method for PID control," *J. Process Control*, vol. 14, no. 6, pp. 635–650, Sep. 2004.
- [41] D. Dasgupta and Z. Michalewicz, *Evolutionary Algorithms in Engineering Applications*. Berlin, Germany: Springer, 2013.
- [42] R. Storn, "On the usage of differential evolution for function optimization," in *Proc. North Amer. Fuzzy Inf. Process.*, Berkeley, CA, USA, Jun. 1996, pp. 519–523.
- [43] S. Das and P. N. Suganthan, "Differential evolution: A survey of the state-of-the-art," *IEEE Trans. Evol. Comput.*, vol. 15, no. 1, pp. 4–31, Feb. 2011.

- [44] M. T. Hagan and M. B. Menhaj, "Training feedforward networks with the Marquardt algorithm," *IEEE Trans. Neural Netw.*, vol. 5, no. 6, pp. 989–993, Nov. 1994.
- [45] B. Mohanty, S. Panda, and P. K. Hota, "Controller parameters tuning of differential evolution algorithm and its application to load frequency control of multi-source power system," *Int. J. Electr. Power Energy Syst.*, vol. 54, pp. 77–85, Jan. 2014.



JABER ALSHEHRI received the B.S. degree in electrical engineering from the King Fahd University of Petroleum and Minerals (KFUPM), Saudi Arabia, in January 2016, where he is currently pursuing the M.S. degree in electrical engineering specializing in power. He joined National Grid-SA, in May 2016, where he is a Protection Engineer with the Protection Engineering Department. He holds an Electrical Engineering practicing license from the Saudi Council of Engineers.

His research interests include power system planning, smart self-healing systems, intelligent control algorithms, power quality improvement of microgrid systems, artificial neural networks, microgrid systems, renewable energy, energy storage systems, power system protection, and smart grids. He has been serving as a Treasurer of the IEEE Power and Energy Society (PES), Saudi Chapter.



MUHAMMAD KHALID received the Ph.D. degree in electrical engineering from the School of Electrical Engineering and Telecommunications (EE&T), University of New South Wales (UNSW), Sydney, Australia, in 2011, where he was a Postdoctoral Research Fellow for three years, and then, he continued as a Sr. Research Associate with the School of EE&T, Australian Energy Research Institute, for another two years. He is currently an Assistant Professor with the

Electrical Engineering Department, King Fahd University of Petroleum and Minerals (KFUPM), Dhahran, Saudi Arabia. He is also a Researcher with the K.A.CARE Energy Research and Innovation Center. He has authored/coauthored several journal and conference papers in the field of control and optimization for renewable power systems. His current research interests include the optimization and control of battery energy storage systems for large-scale grid-connected renewable power plants (particularly wind and solar), distributed power generation and dispatch, hybrid energy storage, EVs, and smart grids.

Dr. Khalid was a recipient of a Highly Competitive Postdoctoral Writing Fellowship from UNSW, in 2010. Most recently, he has received a prestigious K.A.CARE Fellowship. In addition, he has been a Reviewer for numerous international journals and conferences.

...